Magnetocardiogram measurement using SQUID magnetometer and Magneto-Impedance sensor

K. Kobayashi[1], M. Iwai[1], T. Tanaka[2], Y. Hata[2], Y. Ogata[2], B. Kakinuma[2]

[1]Iwate University,   [2]Advantest Laboratories Limited

Magnetocardiogram (MCG) is useful for a clinical application and a health monitoring because it's possible to measure the heart activity without contact. In generally, MCG measurement was used a SQUID magnetometer. For daily health monitoring applications, MCG measurement devices need to be easy to handle. Specifically, it is highly desirable that operations in easy handing, without liquid helium and a magnetically shielded room (MSR). The SQUID magnetometer is high cost of equipment, high running cost due to the liquid helium and necessity of a MSR. On the other hand, A magneto- impedance (MI) sensor can use in room temperature and has a low noise level theoretically [1], [2]. Then we developed 64 channels MI sensor system for MCG measurement. We demonstrate MCG signals measured the SQUID magnetometer and the MI sensor.

MCG measurement for the SQUID magnetometer [3] was performed inside the MSR. The data among 150 trials were averaged for reduction noise. This averaged data is used as the reference signal, because it is high SNR MCG signal. MCG measurement for the MI sensor was performed outside the MSR. The minimum interval between the MI sensor and the chest wall of a normal subject was 5 mm. Noise rejection was carried out by time and spatial average using 64 position data. For time average, all magnetic data were averaged using among 300 trials at each position. For spatial average, 64 position data was compressed into 36 position data. As a result, MCG waveforms of 36 channels in Fig. 1 were obtained, and the QRS complex and T wave could be shown clearly. Compared to the reference signal measured with the SQUID magnetometer, similar characteristics were obtained for the signal measured with the MI sensor. The developed MI sensor system is effective in the health monitoring application.

This study was approved by the Ethics Committee of the Iwate Medical University (No. H22–147) and that of the Iwate University (No. 201704).

Reference
1) L. V. Panina and K. Mohri, Appl. Phys. Lett. **65 (9)** (1994) 1189.
2) L. G. C. Melo, D. Menard, A. Yelon, L. Ding, S. Seaz and C. Dolabdjian, J. Appl. Phys. **103** (2008) 033903.
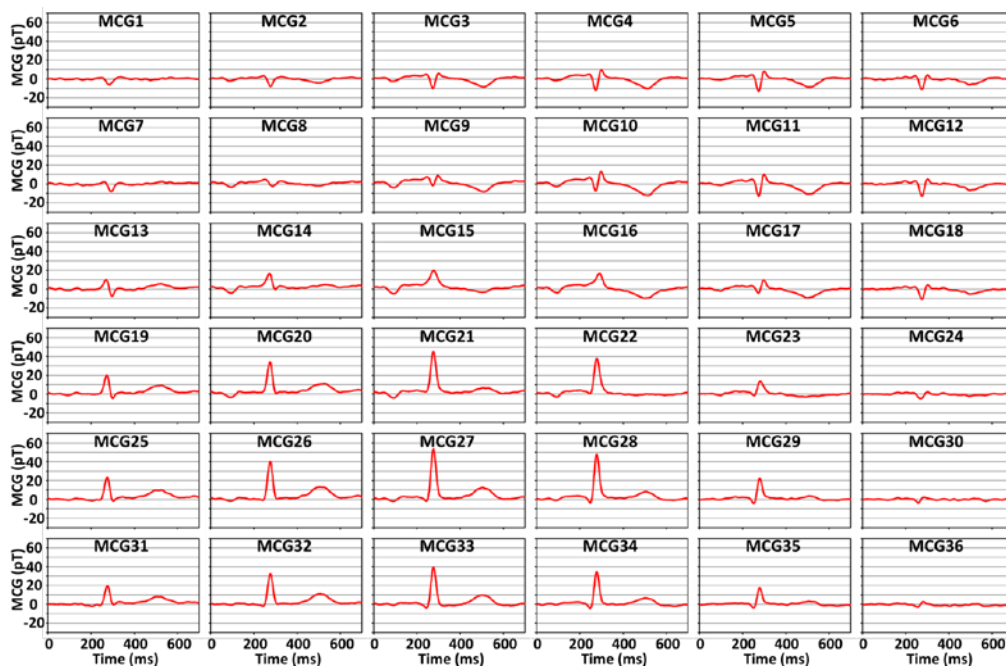3) M. Yoshizawa *et al.*, Phys. C., **426** (2005) 1572.

Fig.1 36ch MCG waveforms after time and spatial averaging.

Recent Progress of Biomagnetic Field Sensors with Ferromagnetic Tunnel Junctions

Yasuo Ando

(Department of Applied Physics, Graduate School of Engineering, Tohoku University)

The discovery of large tunnel magneto-resistance (TMR) effect at room temperature (RT) in magnetic tunnel junctions (MTJs) spurred intensive investigation of MTJ applications for spintronics devices. For sensor application, high sensitivity, low power consumption, small device size and low cost make it prime candidate of the next generation magnetic field sensor such as a bio-magnetic field sensor [1,2]. It needs individual MTJs with a large sensitivity over 10%/Oe and 100 x 100 integrated MTJs to achieve enough output signal and S/N ratio. Here, sensitivity is defined as TMR-ratio/2Hk, where Hk is anisotropy field of the free layer. SQUID is currently the most sensitive of the magnetic sensor and is used for the measurement of biological fields. The sensor with MTJs has much advantage, in particular, the device can operate without liq. He, that is, the sensor can be used at room temperature. Therefore, we expect that the device can have wide application. We prepared the biomagnetic field measurement sensor with a magnetic tunnel junction (MTJ) microfabricated in series and parallel in order to reduce device noise and a magnetic field sensor module incorporating various circuits such as a bridge, an amplifier, a filter, etc., for improving the S / N ratio was fabricated. Using this module, a cardiac magnetic field was successfully measured. In addition, by canceling the environmental noise using two sensor probes, it was shown that a signal can be detected even outside the magnetic shield. In this presentation, we show the detailed characteristics of this sensor. The necessary technical challenges toward its realization and the feasibility in the future are discussed

Reference
1)　K. Fujiwara, M. Oogane, T. Nishikawa, H. Naganuma and Y. Ando, Jpn. J. Appl. Phys., 52, 04CM07 (2013).
2)　D. Kato, M. Oogane, K. Fujiwara, T. Nishikawa, H. Naganuma, and Y. Ando, Appl. Phys. Express, 6, 103004 (2013) ..

Evaluation of harmonic magnetization properties of clinical magnetic nanoparticles for magnetic particle imaging

Takashi Yoshida, Satoshi Ota[*], Takuru Nakamura, Ryoji Takeda[**], Yasushi Takemura[**], Ichiro Kato[***],
Satoshi Nohara[***], and Keiji Enpuku

Department of Electrical Engineering, Kyushu University, Fukuoka, Japan

[*] Department of Electrical and Electronic Engineering, Shizuoka University, Hamamatsu, Japan

[**] Department of Electrical and Computer Engineering, Yokohama National University, Yokohama, Japan

[***] The Nagoya Research Laboratory, Meito Sangyo Co. Ltd., Kiyosu, Japan

1. Introduction

Magnetic nanoparticles (MNPs) have been widely studied due to their potential use in biomedical applications such as drug delivery, hyperthermia and magnetic particle imaging (MPI). Recently, MPI is attracting extensive attention as a new modality for imaging the spatial distribution of MNPs [1]. In this paper, we first overview the basic principle of MPI and MPI scanner. We then evaluate the harmonic magnetization properties, which are directly related to the sensitivity and spatial resolution in MPI, of clinical MNPs.

2. MPI scanner and Magnetic Nanoparticles

MPI, which was first proposed by Gleich and Weizenecker in 2005, is a new modality for the imaging of the spatial distribution of MNPs, especially for in-vivo diagnostics [1]. In MPI, harmonic magnetizations of MNPs under an AC excitation field are sensitively detected to avoid interference between the excitation field and detection coil. To achieve MPI images with a high spatial resolution, a DC gradient field (selection field), which generates the field free point (FFP), as well as an AC excitation field (drive field) are used. MNPs located around FFP generate rich harmonic magnetizations since relatively large AC excitation field and small or zero DC field are applied. On the other hand, all other MNPs located far from the FFP do not generate harmonic magnetizations since they are exposed to large static field. Thus, high spatial resolution can be achieved by scanning the FFP though field of view (FOV). So far, two MPI scanners have been commercialized [2,3]. Figure 1 shows an MPI scanner developed in Kyushu University. The setup is composed of an AC coil for drive field, Nd-Fe-B permanent magnets for selection field, and pickup coil. The amplitude and the frequency of the uniform AC drive field is 3.5 mT and 3 kHz, respectively. The strengths of gradient selection field are 1 and 2 T/m for x- and y-directions, respectively. The third harmonic magnetization from MNPs located around FFP is detected via pickup coil as an MPI signal.

Experiments were performed using water-based maghemite nanoparticles (CMEADM-004, CMEADM-023, CMEADM-033, and CMEADM-033-02). These nanoparticles were supplied by Meito Sangyo Co. Ltd., Kiyosu, Japan. These MNPs were coated by carboxymethyl-diethylaminoethyl dextran, and their core and hydrodynamic diameters are listed in Table 1. Carboxymethyl-diethylaminoethyl dextran-coated iron oxide nanoparticles are negatively charged and are used as a blood-pooling contrast agent [4].
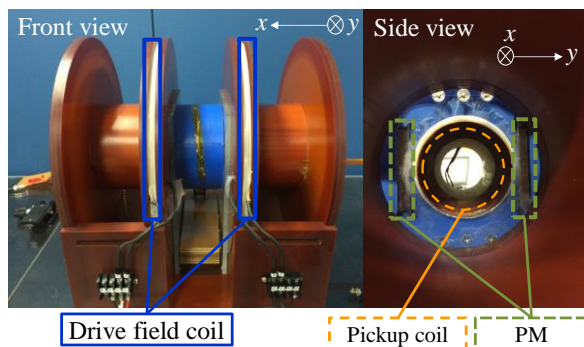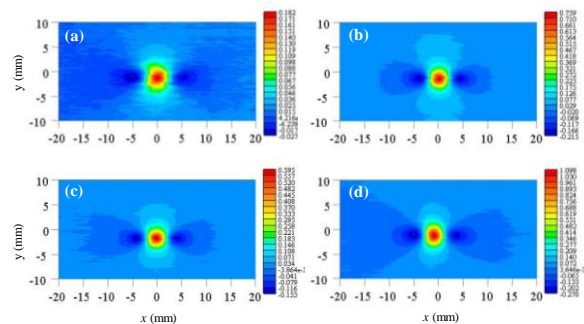

Fig. 1   MPI scanner.

Fig. 2   2D MPI images of the (a) I:CMEADM-004, (b) II:CMEADM-023, (c) III:CMEADM-033, and (d) IV:CMEADM-033-02.

3. Results and Discussion

Figure 2 shows the intensity of the third harmonic magnetization (MPI signal) map of each sample when the sample was mechanically scanned. The FFP is located at the center of each map. The value of maximal intensity and the full width at half maximum (FWHM) of the MPI signal are listed in Table 1. These values are normalized by those of Sample I. The maximal third harmonic intensity of Sample II was higher than that of Samples I and III because the core diameter, d_c, of Sample II is larger than those of Samples I and III [5]. The measured MNP samples are composed of the particles divided into three types of the structures such as the single-core, multi-core, and chain [5]. In particular, the multi-core structure promotes the magnetization and third harmonic signal because of the large size of the effective core [6]. The typical effective core sizes, d_{c_eff}, estimated from the static M-H curves are listed in Table 1. The third harmonic intensity of Sample IV was higher than that of Sample II whereas d_c is smaller than that of Sample II. This indicates that large portion of Sample IV is composed of multi-core particles with large d_{c_eff}. Actually, Sample IV was prepared by collecting the MNPs with large d_{c_eff} by magnetic separation from Sample III [5]. This can be found from the value of d_{c_eff} for Sample IV, i.e., 21.3 nm.

In Table 1, the third harmonic magnetization normalized by the fundamental magnetization, M_3 / M_1, is listed. For the estimation of M_3 / M_1, the AC magnetization signal was measured when an excitation field intensity of 10 mT and frequency of 10 kHz was applied. The measurements and estimations of M_3 / M_1 were performed at Yokohama National University and Shizuoka University. As shown in Table I, the FWHM correlates with the M_3 / M_1. Sample IV shows the highest M_3 / M_1 and the smallest FWHM among all four samples. In particular, M_3 / M_1 of Sample III was higher than that of Sample II and the FWHM of Sample III was smaller than that of Sample II, although the maximal intensity of the MPI signal of Sample III was lower than that of Sample II. It suggests that the difference in the structures of Samples II and III influences the maximal intensity and the FWHM of the MPI signal.

Table 1 Parameters of measured MNP samples. Effective core size d_{c_eff} was estimated from static M-H curve. Maximal intensity of MPI signal and FWHM were normalized by those of Sample I:CMEADM-004.

Sample # : Measured MNP	d_c (nm)	d_{c_eff} (nm)	d_h (nm)	Maximal intensity of MPI signal	FWHM	M_3 / M_1
I : CMEADM-004	4	5.4	38	1	1	0.0728
II: CMEADM-023	8	7.4	83	3.9	0.86	0.0975
III: CMEADM-033	5-6	5.6 (21.3)	54	3.1	0.81	0.115
IV: CMEADM-033-02	6	21.3	64	6.1	0.76	0.123

4. Conclusions

In this paper, we first overviewed the basic principle of MPI and MPI scanner. We then evaluated the third harmonic magnetization (MPI signal) properties of clinical MNPs. We showed that MNP sample with appropriate core size generates large MPI signal. We also showed that the FWHM, which is directly related to the spatial resolution of the MPI image, correlates with the M_3 / M_1.

Reference
1) B. Gleich and J. Weizenecker. *Nature*, **435**, 1217 (2005).
2) https://www.bruker.com/jp/products/preclinical-imaging/magnetic-particle-imaging-mpi/overview.html
3) https://www.magneticinsight.com/momentum-imager/
4) N. Nitta, K. Tsuchiya, A. Sonoda, S. Ota, N. Ushio, M. Takahashi, K. Murata, and S. Nohara, *Jpn. J. Radiol*, **30** (10), 832—839 (2012).
5) S. Ota, R. Takeda, T. Yamada, I. Kato, S. Nohara, and Y. Takemura, *Int. J. Magn. Part. Imaging*, **3**, 1703003 (2017).
6) T. Yoshida, N. B. Othma n, and K. Enpuku, *J. Appl. Phys.*, **114**, 173908 (2013).

Sentinel lymph node biopsy using magnetic nanoparticles and magnetic probe

M. Kusakabe[1,2], H. Takei[3], S. Nakamura[4] and M. Sekino[5]

[1] Graduate School of Agricultural and Life Sciences, The University of Tokyo, Tokyo, Japan

[2] Matrix Cell Research Institute Inc., Ibaraki, Japan

[3] Department of Breast Oncology, Nippon Medical School Hospital, Tokyo, Japan

[4] Division of Breast Surgical Oncology, Department of Surgery, Showa University Hospital, Tokyo, Japan.

[5] Graduate School of Engineering, The University of Tokyo, Tokyo, Japan

In surgery for early breast cancer, it is important that much less invasive breast conservation therapy is done and that axillary lymph node dissection is avoided to increase the patient's quality of life (QOL). For this purpose, a sentinel lymph node biopsy (SLNB) has been established to determine the sentinel lymph node (SLN) in which lymph fluid containing cancer cells from a tumor first flowed.

With the current method using radioisotopes (RIs), 99mTc phytic acid is subcutaneously injected into the areola one day prior to surgery. On the following day, the SLN that contains the radioactive tracer is detected with a radiation detector and is excised. However, RIs not only directly radiate patients but also require specific radiation control areas, making it difficult to implement in small and medium hospitals.

To solve this problem, novel methods for detecting a SLN by using a non-RI tracer such as dye (patent blue) or fluorescence (indocyanine green: ICG) have been used. However, the results of these methods are subjective, and the methods have the problem of having low detection rates.

In my presentation, we introduce a novel system for breast SNLB that uses a magnetic probe developed by us and magnetic nanoparticles (ferucarbotran).

References
1)　M. Shiozawa *et al.*, Breast Cancer. 20(3) (2012) 223-229.
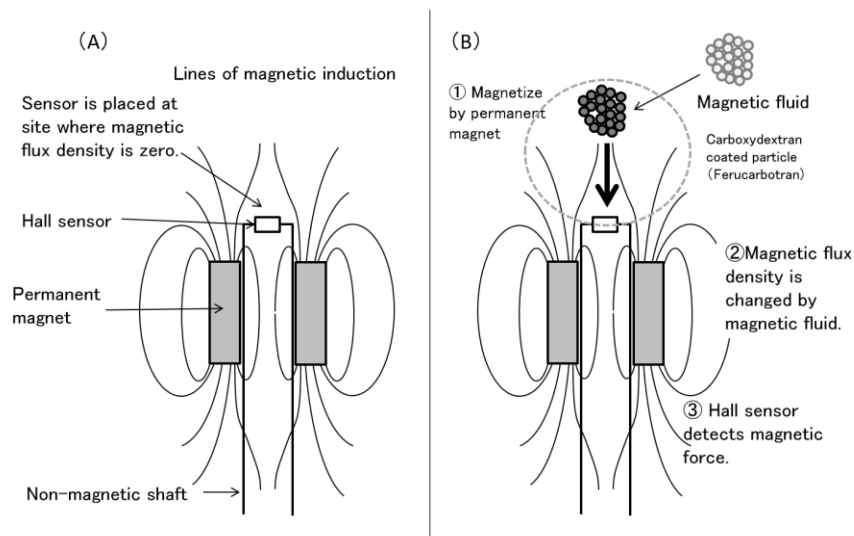2)　M. Sekino *et al.*, Sci. Rep. 19;8(1)(2018) 1195.
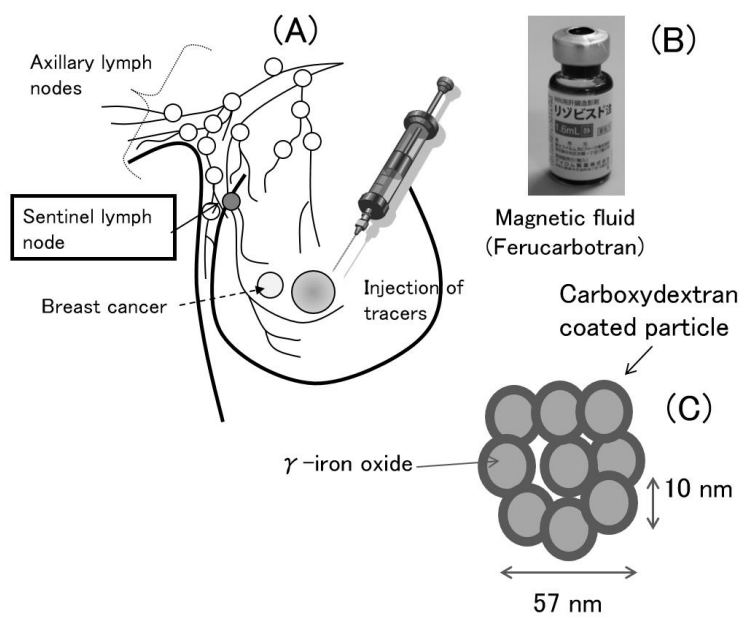

Fig. 1 Measurement principle of magnetic probe.

Fig. 2 SLN detection method using magnetic particles.

Development of transcranial magnetic stimulator for treatments of neurological and psychiatric diseases at home

Masaki Sekino[1,2], Koichi Hosomi[2], and Youichi Saitoh[2]

[1]Graduate School of Engineering, the University of Tokyo, [2]Graduate School of Medicine, Osaka University

Transcranial magnetic stimulation (TMS) has been applied to diagnosis of neurological diseases and to basic neuroscience studies since this technique was demonstrated for the first time in 1985. The applications are now extending to cover treatments of neurological and psychiatric diseases such as depression, neuropathic pain, and Parkinson's disease[1]. A magnetic stimulator for treatment of depression was approved last year in Japan. Previous studies suggest that the therapeutic effects are attributed to neuromodulation caused by repetitive TMS at more than 1 pulses per second. In order to maintain the therapeutic effects, patients have to undergo TMS every day. Such treatment will be widely available if a compact magnetic stimulator which can be installed in patients' home is developed. Improvement of efficiency in producing magnetic fields should be improved for downsizing the stimulator system. In addition, the therapeutic effect is affected by the positioning error of stimulator coil. Our group is developing novel TMS techniques including highly efficient stimulator coil and a coil with improved robustness against positioning error.

In order to increase the efficiency of inducing electric fields in the brain, we proposed an eccentric figure-eight coil[2]. As shown in figure 1, the coil consists of a pair of eccentric spirals, and the center of each spiral is shifted toward the middle of the coil. Because the conductor is dense at the middle of the coil, induced electric field increases. This means that the electric field for exciting neurons can be induced with smaller coil currents. Numerical simulations were conducted for optimizing the designing parameters such as inner and outer radii and number of turns. A prototype coil was fabricated based on these optimized parameters. Stimulation of human motor cortex using the prototype coil showed that the neurons were activated with significantly lower coil currents compared with a conventional concentric figure-eight coil. Another study showed that the efficiency is further improved when the eccentric spirals are formed on the surface of a sphere conforming to the surface of the head.

Because the size of stimulating spot for figure-eight coil is as small as 5 mm, precise and reproducible positioning of the coils is necessary for obtaining stable therapeutic effect. This requirement of precision can be reduced if the spot of stimulation is enlarged. We proposed a bowl-shaped coil which exhibit an enlarged distribution of induced field compared with a conventional figure-eight coil[3]. Coil conductors are aligned in parallel over the target area in the brain. The return conductors are placed above these parallel conductors to form coil loops. Numerical simulations showed that the bowl-shaped coil exhibits an enlarged distribution of induced electric field. One of the technical challenges is larger coil current for stimulating neurons. Improvement of coil design is necessary for balancing the robustness against positioning error and the high efficiency of stimulation.

Figure 1 (a) Concentric figure-eight coil and (b) eccentric figure-eight coil[2].

Reference

1) Hirayama A, Saitoh Y, Kishima H, Shimokawa T, Oshino S, Hirata M, Kato A, Yoshimine T. 2006. Reduction of intractable deafferentation pain by navigation-guided repetitive transcranial magnetic stimulation of the primary motor cortex. Pain 122:22-27.

2) M. Sekino, H. Ohsaki, Y. Takiyama, K. Yamamoto, T. Matsuzaki, Y. Yasumuro, A. Nishikawa, T. Maruo, K. Hosomi, and Y. Saitoh, "Eccentric figure-eight coils for transcranial magnetic stimulation,"Bioelectromagnetics, vol. 36, pp. 55-65, 2015.

3) K. Yamamoto, M. Suyama, Y. Takiyama, D. Kim, Y. Saitoh, and M. Sekino, "Characteristics of bowl-shaped coils for transcranial magnetic stimulation," Journal of Applied Ph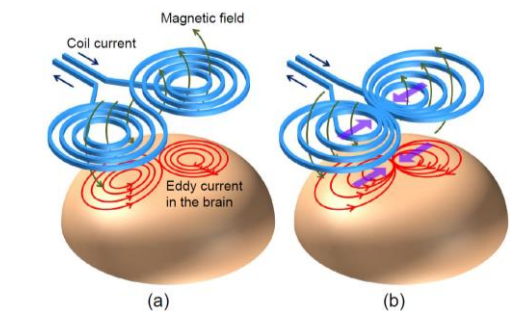ysics,vol. 117, No.17, 17A318 , 2015.